PLOS ONE

Plasma metabolomic study in perinatally HIV-infected children using 1H NMR spectroscopy reveals perturbed metabolites that sustain during therapy
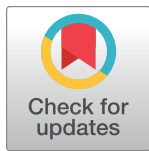
Urvinder Kaur S.[1]☯, Bolaji Fatai Oyeyemi[2]☯¤, Anita Shet[3], Bindu Parachalil Gopalan[4,5], Himanshu D.[6], Neel Sarovar Bhavesh[2], Ravi Tandon[1]*

1 Laboratory of AIDS Research and Immunology, School of Biotechnology, Jawaharlal Nehru University, New Delhi, India, 2 Transcription Regulation Group, International Centre for Genetic Engineering and Biotechnology (ICGEB), New Delhi, India, 3 International Vaccine Access Center, Johns Hopkins School of Public Health, Baltimore, MD, United States of America, 4 Division of Infectious Diseases, St. John's Research Institute, St. John's National Academy of health Sciences, Bangalore, India, 5 School of Integrative Health Sciences, University of Trans-Disciplinary Health Sciences and Technology (TDU), Bangalore, India, 6 Department of Medicine, King Georges Medical University, Lucknow, India

☯ These authors contributed equally to this work.
¤ Current address: Molecular Biology Research Group, Department of Science Technology, The Federal Polytechnic Ado-Ekiti, Ado Ekiti, Nigeria
* ravitandon@jnu.ac.in

Abstract

Background

Perinatally HIV-infected children on anti-retroviral treatment (ART) are reported to have metabolic abnormalities such as dyslipidemia, lipodystrophy, and insulin resistance which potentially increase the risk of diabetes, kidney, liver and cardiovascular disease.

Objective

To elucidate HIV-mediated metabolic complications that sustain even during ART in perinatally HIV-infected children.

Method

We have carried out metabolic profiling of the plasma of treatment-naïve and ART-suppressed perinatally HIV-infected children and uninfected controls using 1H nuclear magnetic resonance (NMR) spectroscopy followed by statistical analysis and annotation.

Result

Validated multivariate analysis showed clear distinction among our study groups. Our results showed elevated levels of lactate, glucose, phosphoenolpyruvic acid, propionic acid, 2-ketobutyric acid and tricarboxylic acid (TCA) cycle metabolites in untreated HIV-infected children compared to uninfected controls. ART normalized the levels of several metabolites, however the level of lactate, phosphoenolpyruvic acid, oxoglutaric acid, oxaloacetic acid,

myoinositol and glutamine remained upregulated despite ART in HIV-infected children. Pathway analysis revealed perturbed propanoate metabolism, amino acid metabolism, glycolysis and TCA cycle in untreated and ART-suppressed HIV-infected children.

Conclusion

Developing therapeutic strategies targeting metabolic abnormalities may be beneficial for preventing diabetes, cardiovascular disease or other associated complications in perinatally HIV-infected children.

Introduction

According to UNAIDS report 2019, there are approximately 1.7 million children less than 15 years old living with HIV worldwide and 160000 children became newly infected [1]. Maternal-to-child transmission (MTCT) accounts for more than 90% of pediatric HIV infection [2]. In the era of antiretroviral therapy (ART), the disease progression has been controlled and the life expectancy of HIV-infected children has greatly increased [3]. However, with an expanded life span, HIV-infected children have high prevalence of metabolic abnormalities such as dyslipidemia, lipodystrophy and insulin resistance, which potentially increases the risk of early cardiovascular atherosclerosis, kidney failure, and diabetes in this population [4, 5]. Several factors including HIV [6, 7], host immune response [8] and ART [4, 9] contribute to these metabolic complications.

Previous study demonstrated that prolonged exposure to protease inhibitors (PIs) in HIV-infected children was associated with lipid abnormalities and lipodystrophy [10]. The use of ART and persistent inflammation in children living with HIV were shown to be associated with increased carotid intima media thickness, which is a marker of cardiovascular disease (CVD) [11]. In HIV-infected children, increased use of ART also reported to cause dyslipidemia and insulin resistance [12, 13]. Thus, metabolic abnormalities in perinatally HIV-infected children are of great concern since ART is given early in life. However, even before the introduction of ART alterations in lipid metabolism and sensitivity to insulin were reported during HIV infection [14]. A recent study showed increased cardiovascular abnormalities in HIV-infected children without ART(treatment-naïve) [6]. Since existing clinical indicators of HIV are not infallible, observing the development of HIV infection in children and monitoring their responses to ART using NMR metabolic profiling will be germane in the identification of novel biological markers. Several studies had focused on the impact of ART on metabolism in perinatally HIV-infected children [3, 4, 6, 15, 16], metabolic complications due to HIV in treatment-naïve HIV-infected children is less understood. It is thus imperative to monitor metabolic state of children with or without ART.

Metabolomics is an unbiased method to identity and quantify metabolites present in the biological fluids and tissues, providing the metabolic fingerprint of an organism. Metabolomics helps to determine metabolic alterations during various diseases like coronary heart disease [17], colon cancer [18] and hepatitis [19] and has been used to discover novel clinical biomarkers and therapeutic targets.

The NMR spectroscopy was first used by Hewer et al. to profile metabolites in the serum of chronically HIV-infected adults. They demonstrated a distinction in the sera among treatment-naïve, ART-suppressed (ART-experienced and virologically suppressed) HIV-infected subjects and HIV negative controls [20]. Since then, other studies have used NMR and MS to

demystify metabolic response to HIV in adults [21–23]. Moreover, it is also necessary to comprehensively study HIV-infected children plasma metabolic profile as they have remarkable difference in HIV-disease progression with higher viremia compared to HIV-infected adults [24, 25] and also have metabolic abnormalities [4, 5]. In this study, we performed untargeted metabolic profiling of treatment-naïve and ART-suppressed perinatally HIV-infected children and compared them to age-matched uninfected controls by using 1H NMR spectroscopy.

Material and methods

Study participants

This pilot cross-sectional study included 30 perinatally HIV-infected children and 12 age-matched uninfected controls who had been recruited in June 2016 from the south part of India. All the children were less than 15 years old. Perinatal infection was confirmed by the documentation of HIV infection in children within 1 year of life along with documentation of maternal HIV infection. Among HIV-infected children, 15 children were on ART for more than 6 months, whereas the other 15 children were not on ART (treatment-naïve). Those on ART had undetectable plasma viral load (VL < 50 copies/ml) and 60% of them were receiving a combination of Zidovudine (ZDV), Lamivudine (3TC) plus Nevirapine (NVP), 20% were receiving Atazanavir (ATV), 3TC plus Efavirenz (EFV), 13% were receiving Stavudine (d4T), 3TC plus NVP and the remaining 7% were receiving ZDV, 3TC plus Lopinavir/Ritonavir (LPV/r). Uninfected controls were matched with the HIV-infected children for age and sex. Children with age greater than 15, with co-infections such as tuberculosis or viral hepatitis and metabolic abnormalities were excluded from this study. All study participants belonged to same ethnicity, geographical area and had similar dietary habits. This study was approved by Institutional Review Board (IRB) of St. Johns Medical College & Hospital at Bangalore, Jawaharlal Nehru University (JNU) at New Delhi and King George's Medical University (KGMU) Lucknow, and was carried out in accordance with the approved guidelines. The biosafety approval was obtained from Institutional Biosafety Committee (IBSC) of JNU for handling plasma samples. Informed written consent was obtained from parents/guardian of all the children who participated in our study. The characteristics of subjects are listed in Table 1.

Plasma viral load and CD4 count. Plasma HIV-1 viral load (VL) was measured using Abbott Real Time HIV-1 assay with a lower limit of detection of 50 copies of RNA/ml (Abbott Molecular Inc., Des Plaines, IL, USA). CD4 T cell count was measured using FC500™ flow cytometer (Beckman Coulter, Fullerton, California, USA).

Table 1. Subjects characteristics.

Parameters	Treatment naïve HIV-infected children	ART-suppressed HIV- infected children	HIV negative controls
Number	15	15	12
Age (years)	10 (8–12)	11 (9–11)	10 (8–11)
CD4 count (cells per ul)	615 (423–749)	1157(594–1336)	1338 (1112–1449)
Plasma viral load (HIV RNA copies per ml)	28,410 (10,842–60,193)	< 50	NA
ART regimens	NA	ZDV+3TC+NVP (60%)	NA
		ATV+3TC+EFV (20%)	
		d4T+ 3TC+ NVP (13%)	
		ZDV+ 3TC+ LPV/r (7%)	

Values are shown as median (IQR), NA: Not applicable.

Sample collection. Peripheral blood was collected into vacutainer blood collection tubes containing EDTA and whole blood was centrifuged to isolate plasma. Plasma samples were stored at -80˚C for NMR metabolic profiling.

Sample preparation and NMR spectroscopy

Plasma samples were thawed on ice and centrifuged at 10,000g for 10 min to remove particulates. 70 μL of supernatant was then taken and immediately added to 140 μL of 0.1M potassium phosphate buffer (composition: 0.2M of K_2HPO_4 and KH_2PO_4, 10% 4,4-dimethyl-4-silapentane-1-sulfonic acid (DSS), D_2O, pH 7.4). The mixture was transferred to an NMR tubes (outer diameter: 3.0 mm) for NMR analysis. NMR experiments were performed at 298K on a Bruker 500.13 MHz AVANCE III spectrometer equipped with 5mm triple-resonance z-gradient cryoprobe (CPTCI 1H–31P/13C/2D Z-GRD). TopSpin, version 3.5 (Bruker Corporation), was used for spectrometer control. Temperature was calibrated using a 100% d4-methanol sample. [1]H Carr–Purcell–Meiboom–Gill (CPMG) echo sequence was used to record NMR spectra. A total CPMG delay of 300 ms was used with an echo time of 200 μs was used based on experimental optimization. NMR spectra were obtained with 32 scans and a relaxation delay of 4 sec. Free induction decays (FIDs) 10,000 Hz spectral width and 3.33 sec acquisition time were collected for each sample.

NMR data processing

NMR data processing was done using Topspin, version 3.5. Automatic matching, tuning and shimming of each data were done. They were Fourier transformed after zero-filling to varying points and application of a line-broadening factor of 0.30 Hz. Consequently, NMR spectra were phased and automatically baseline corrected. Spectra were referenced to DSS at 0 ppm and spectral region between 4.5 and 4.7 ppm was set to zero to remove water resonance suppression effect. Peaks for each samples were picked and each NMR peak list and intensity data were then imputed into Metaboanalyst 3.0. This program groups peaks based on their ppm values using a moving window of 0.03 ppm and a step of 0.015 ppm and peaks within the same group were aligned to their median ppm. Peaks appearing in less than half of the samples were excluded from downstream analysis.

Statistical analysis, metabolite identification and pathway analysis

MetaboAnalyst 3.0 (http://www.metaboanalyst.ca/) was used for statistical analyses and NMR spectral annotations [26]. This is a web server with numerous statistical and machine learning algorithms for comprehensive metabolomics data analysis, visualization, and interpretation. Processed raw data from TopSpin were log transformed, normalized by sample median and auto-scaled by mean-centering and dividing by the standard deviation of each variable for better, reliable and accurate biological inference before univariate and multivariate data analysis in Metaboanalyst 3.0 [27].

Supervised and unsupervised multivariate statistical analysis including principal component analysis (PCA), partial least squares-discriminant analysis (PLS-DA) and orthogonal partial least squares-discriminant analysis (OPLS-DA) were performed to discriminate between our study groups. Metabolites responsible for difference in the metabolic profiling were obtained from variable importance in projection plot (VIP) of threshold 1.0 in PLS-DA. Both PLS-DA and OPLS-DA models were validated for predictability and PLSDA: R^2, accuracy, Q^2 and OPLS-DA: R^2Y and Q^2 were generated to confirm whether the difference between our study groups was statistically significant. One-way analysis of variance (ANOVA) was employed to analyze the significance of differential metabolites across our study groups.

Corresponding metabolites for differential peaks were identified from NMR spectra databases which include Human Metabolome Data Bank (HMDB) [28] and complex mixture analysis (COLMAR) query web server [29] as listed in Table 2. These metabolites were checked with two-dimensional (2D) homonuclear ^{1}H-^{1}H J-resolved experiments and compared with previously published one and two dimentional values [18, 20, 22]. The representative 500 MHz 1H-1H J-Resolved (JRes) spectrum is shown in S1 Fig. Metabolic pathway analysis was carried out using MetaboAnalyst 3.0 [26], Kyoto Encyclopedia of genes and genomes (KEGG) [30] and HMDB pathway.

Results

Multivariate analysis distinguishes plasma metabolic profile among treatment-naïve, ART-suppressed perinatally HIV-infected children and uninfected controls

A representative one dimensional ^{1}H-NMR spectra of plasma from treatment-naïve, ART-suppressed perinatally HIV-infected child and uninfected control is depicted in Fig 1.

To determine whether it was possible to differentiate HIV-infected children from uninfected controls on the basis of the NMR spectra, we carried out unsupervised multivariate analysis such as PCA and supervised multivariate analysis such as PLS-DA and OPLS-DA. PCA score plot showed that treatment-naïve HIV-infected children could be distinguished from ART-suppressed HIV-infected children and uninfected controls (Fig 2A). Whereas PLS-DA score plot revealed excellent separation among treatment-naïve, ART-suppressed perinatally HIV-infected children and controls (Fig 2B and 2C). On validation by permutation tests, we obtained PLS-DA model with accuracy 0.972 (R^2 = 0.990 and Q^2 = 0.919) and p = 0.02 and OPLS-DA with R^2Y = 0.979 and Q^2 = 0.917. For biological data, a model with R^2 = 0.7 and Q^2 = 0.4 is considered to be good.

Perturbed levels of metabolites in HIV-infected children despite suppressive therapy

To identify the metabolites with the highest degree of differences in the metabolomes among treatment-naïve, ART-suppressed HIV-infected children and uninfected controls, we used PLS-DA to evaluate variable importance in projection (VIP) scores. A heatmap showing relative intensity of some metabolites as identified by VIP scores (Fig 3). We identified 66 metabolites to be significantly altered in untreated HIV-infected children when compared to uninfected controls. Out of these, the levels of 38 metabolites were significantly high in untreated HIV-infected children compared to controls, while 28 metabolites were significantly low in untreated HIV-infected children compared to controls (S1 Table).

Insulin resistance is one of the major metabolic disorders seen in patients living with HIV [31]. Within altered metabolites, the levels of lactate, glucose, phosphoenol pyruvic acid and TCA cycle metabolites such as succinic acid, oxoglutaric acid, and oxaloacetic acid were significantly higher in the plasma of treatment-naïve HIV-infected children compared to uninfected controls. Compared to controls, the plasma levels of some other metabolites like propionic acid, acetate, acetoacetate, myoinositol and trimethylamine-N-oxide (TMAO) were significantly elevated whereas 2-ketobutyric acid and choline were siginificantly lowered in treatment-naïve HIV-infected children. treatment-naive HIV-infected children also showed abnormalities at the aminoacid levels with significantly lower plasma level of glycine, sarcosine, serine, tyrosine, valine and higher plasma level of alanine, creatine, glutamine, leucine, methionine and taurine compared to controls (Fig 4 and S1 Table).

Table 2. Nuclear magnetic resonance chemical shift assignments of differential compounds identified in serum of treatment naïve, ART-suppressed and uninfected control.

S/N	Compound	HMDB ID	Chemical shift (ppm)[a]
1	Leucine	HMDB0000687	0.935 (d), 0.947 (d), 1.633 (m), 1.700 (m)
2	Valine	HMDB0000883	0.97 (d), 1.02 (d), 2.23 (m)
3	Propionic acid	HMDB0000237	1.043 (t), 2.170 (q)
4	2-Ketobutyric acid	HMDB0000005	1.069 (t), 2.760 (q)
5	Ethanol	HMDB0000108	1.170 (t), 3.647 (q)
6	β-hydroxybutyrate	HMDB0000011	1.204 (d), 2.314 (dd), 2.414 (dd), 4.160 (m)
7	Caproic acid	HMDB0000535	0.864 (t), 1.274 (m), 1.536 (m), 2.518 (t)
8	Lactate	HMDB0000190	1.32 (d), 4.10 (q)
9	Dimethylmalonic acid	HMDB0002001	1.430 (s)
10	Alanine	HMDB0000161	1.46 (d) 3.77 (q)
11	2-Ethyl-2-Hydroxybutyric acid	HMDB0001975	0.873 (t), 1.670 (m), 1.795 (m)
12	Leucine	HMDB0000687	0.935 (d), 0.947 (d), 1.633 (m), 1.700 (m)
13	Ethylmalonic acid	HMDB0000622	0.889 (t), 1.744 (m), 3.023 (t)
14	Putrescine	HMDB0001414	1.754 (m), 3.040 (t)
15	N6-acetyl-L-lysine	HMDB0000206	1.409 (m), 1.562 (m), 1.871 (m), 1.990 (s), 3.195 (q), 3.740 (t)
16	Acetate	HMDB0000042	1.91 (s)
17	N-acetyl-L-alanine	HMDB0000766	1.315 (d), 2.000 (s), 4.114 (t)
18	Methionine	HMDB0000696	2.12 (s), 2.61 (t)
19	Suberic acid	HMDB0000893	1.296 (s), 1.538 (s), 2.163 (s)
20	Acetone	HMDB0001659	2.22 (s)
21	Acetoacetate	HMDB00060	2.29 (s)
22	Oxaloacetic acid	HMDB0000223	2.377 (s)
23	Succinic acid	HMDB0000254	2.393 (s)
24	Glutamine	HMDB0000641	2.06 (m), 2.38 (m), 3.65 (t)
25	Pyridoxal	HMDB0001545	2.448 (s), 5.038 (d), 5.219 (d), 6.542 (d), 2.448 (s)
26	Citrate	HMDB0000094	2.52 (d), 2.67(d)
27	2,2-Dimethylsuccinic acid	HMDB0002074	1.250 (s), 2.660 (s)
28	Sarcosine	HMDB0000271	2.72 (s), 3.60 (s)
29	Aspartate	HMDB0000191	2.62 (dd), 2.78 (dd), 3.86 (t)
30	Dimethylglycine	HMDB0000092	2.910 (s), 3.710 (s)
31	Oxoglutaric Acid	HMDB0000208	2.428 (m), 2.996 (m)
32	Creatine	HMDB0000064	3.02 (s), 3.92 (s)
33	Ethanolamine	HMDB0000149	3.130 (d), 3.810 (d)
34	Choline	HMDB0000097	3.19 (s)
35	Glycerophosphorylcholine	HMDB0000086	3.200 (s), 3.637 (m), 3.897 (m), 4.305 (m)
36	Trimethylamine N-oxide	HMDB0000043	3.25 (s), 3.89 (s)
37	1,3-Dimethyluric acid	HMDB0001857	3.298 (s), 3.428 (s)
38	Theophylline	HMDB0001889	3.340 (s), 3.535 (s) 7.990 (s)
39	Methylguanidine	HMDB0001522	2.833 (s), 3.366 (s)
40	Taurine	HMDB0000251	3.19 (t), 3.41 (t)
41	Cis-Aconitic acid	HMDB0000072	3.435 (d). 6.580 (s)
42	β–Glucose	HMDB0000122	3.39 (m), 3.46 (m), 3.48 (m), 3.71 (m), 3.89 (m), 4.64 (d)
43	Glycine	HMDB0000123	3.52 (s)
44	Myo-inositol	HMDB0000211	3.54 (dd), 3.63 (t), 4.06 (m)
45	Glucono-1,5-lactone	HMDB0000150	3.666 (dd), 3.767 (m), 3.817 (dd), 4.027 (d), 4.125 (d)
46	N-Methyl-a-aminoisobutyric acid	HMDB0002141	1.590 (s), 3.840 (s)

(Continued)

Table 2. (Continued)

S/N	Compound	HMDB ID	Chemical shift (ppm)[a]
47	Mannitol	HMDB0000765	3.69 (m), 3.88 (m)
48	Serine	HMDB0000187	3.91 (m), 3.77 (m)
49	Isopropyl alcohol	HMDB0000863	1.17 (d), 3.98 (m)
50	6-Phosphogluconic acid	HMDB0001316	3.840 (m), 3.961 (m), 4.095 (m), 4.185 (d)
51	Fructose	HMDB0000660	3.577 (m), 3.695 (m), 3.823 (m), 3.903 (dd), 4.005 (m), 4.029 (dd), 4.118 (m)
52	Glyceric acid	HMDB0000139	3.779 (m), 4.133 (m)
53	Pyridoxamine 5'-phosphate	HMDB0001555	2.461 (s), 4.314 (s), 4.852 (s), 7.645 (s)
54	2,4-Diamino-6hydroxypyrimidine	HMDB0002128	4.953 (s)
55	Phosphoenolpyruvic acid	HMDB0000263	5.180 (t), 5.360 (t)
56	3,4-Dihydroxymandelic acid	HMDB0001866	6.843 (dd), 6.888 (d), 6.918 (d)
57	Tyrosine	HMDB0000158	7.17 (d), 6.86 (d), 2.98 (q)
58	2-Furoylglycine	HMDB0000439	3.935 (d), 6.643 (dd), 7.190 (d), 7.700 (d)
59	Indoxyl sulfate	HMDB0000682	7.209 (dd), 7.281 (dd), 7.362 (s), 7.508 (d), 7.712 (d)
60	4-Pyridoxic acid	HMDB0000017	2.310 (s), 4.510 (s), 7.530 (s)
61	Mandelic acid	HMDB0000703	4.980 (s), 7.380 (m), 7.420 (d)
62	Phenylacetylglycine	HMDB0000821	3.665 (s), 3.744 (d), 7.380 (m)
63	Quinolinic acid	HMDB0000232	7.440 (q), 7.990 (t), 8.430 (t)
64	Formic acid	HMDB0000142	8.440 (s)

[a]Multiplicity: s singlet, d doublet, t triplet, q quartet, dd doublet of doublets, m multiplet.

https://doi.org/10.1371/journal.pone.0238316.t002

In treated children the plasma levels of glucose, propionic acid, 2-ketobutyric acid, succinic acid, acetic acid, acetoacetic acid, TMAO, glycine, sarcosine, tyrosine, valine, alanine, creatine, leucine, methionine, and taurine were restored to the levels found in uninfected controls. However, the plasma levels of lactate, phosphoenolpyruvic acid, oxoglutaric acid, oxaloacetic acid, myoinositol and glutamine remained elevated and the plasma levels of choline and serine remained lowered in treated HIV-infected children suggesting the failure of ART in restoring the levels of these metabolites (Fig 4 and S1 Table).

Metabolic pathway analysis

Metabolites that were significantly altered in treatment-naïve and ART-suppressed perinatally HIV-infected children when compared to controls, were subjected to pathway analysis. We found 22 metabolic pathways among treatment-naïve, ART-suppressed perinatally HIV-infected children and uninfected controls that were significantly modulated (S2 Table). The prominent changes were observed in amino acid metabolism, TCA cycle, glycolysis pathway (Fig 5).

Discussion

In this study, we profiled the plasma metabolome of treatment-naïve and ART-suppressed HIV-infected children, and compared them with that of uninfected controls using NMR spectroscopy. Our data suggests perturbed levels of metabolites in treatment-naïve perinatally HIV-infected children compared to uninfected controls. The ART appears to normalize majority of metabolites in perinatally HIV-infected children under treatment; some metabolites like lactate, phosphoenolpyruvic acid, oxoglutaric acid, oxaloacetic acid, myoinositol and glutamine remain elevated either due to previous exposure to HIV or ART itself.
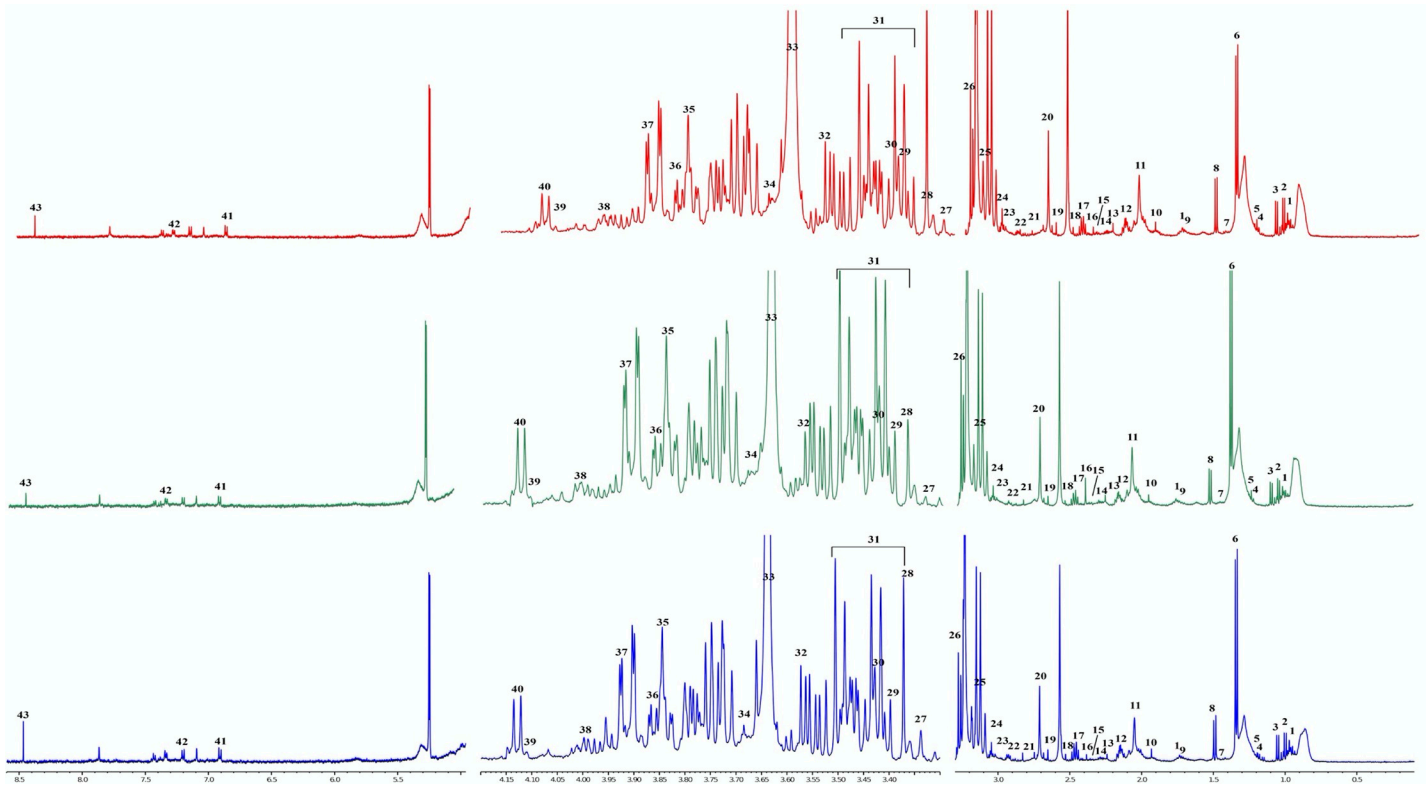
Fig 1. Representative 500-MHz 1H nuclear magnetic resonance spectra of serum from treatment naïve (green), ART-suppressed (green) perinatally HIV-infected child and uninfected control (blue). 1- Leucine, 2- valine, 3–2-Ketobutyric acid, 4- ethanol, 5- β-hydroxybutyrate, 6- lactate, 7- dimethylmalonic acid, 8- alanine, 9–2-ethyl-2-Hydroxybutyric acid, 10- acetate, 11- n-acetyl-L-alanine, 12- methionine, 13- acetone, 14- acetoacetate, 15- oxalacetic acid, 16- succinic acid, 17- glutamine, 18- pyridoxal, 19- citrate, 20- sarcosine, 21- aspartate, 22- dimethylglycine, 23- oxoglutaric acid, 24- creatine, 25- choline, 26- trimetylamine N-oxide, 27- theophylline, 28- methylguanidine, 29- taurine, 30- cis-aconitic acid, 31- β–glucose, 32- glycine, 33- myo-inositol, 34- glucono-1,5-lactone, 35- N-methyl-a-aminoisobutyric acid, 36- mannitol, 37- serine, 38- isopropyl alcohol, 39- fructose, 40- glyceric acid, 41- tyrosine, 42–2-furoylglycine, 43- formic acid. Broken lines indicate excluded spectral region.

Altered metabolites due to perturbed metabolic process might cause metabolic disorders like insulin resistance, hyperlipidemia, obesity and high blood pressure. It was beyond the scope of clinical routine practice and the study scope to measure lipid levels, insulin resistance etc. However, none of the HIV-infected children in this study had high BMI. Previous studies have shown a direct link between perturbed glycolytic pathway and chronic inflammation [32, 33]. Metabolic profiling of plasma of HIV-infected adults had shown higher levels of glucose and lactic acid, which is suggestive of perturbed glycolytic pathway [22]. In our study, the increase in the level of glucose, lactic acid and phosphoenolpyuvic acid among treatment-naïve perinatally HIV-infected children is an indication of perturbed glycolysis and supports the previous findings in HIV-infected adults [22]. In addition, high level of glucose or hyper-glycemia has been known to promote HIV pathogenesis. This was supported by a study which showed that the high glucose increases the expression of CXCR4 in T cells thereby enhancing the entry of HIV into T cells [34]. Glucose metabolism has also been reported to play a major role in interleukin-1β (IL-1β) production [35] and thus high glucose level during chronic HIV infection results in the upregulation of IL-1β level in the plasma of HIV-infected subjects. A study by Mikulak et al showed that IL-1β enhances HIV entry and its persistence in human podocytes [36].
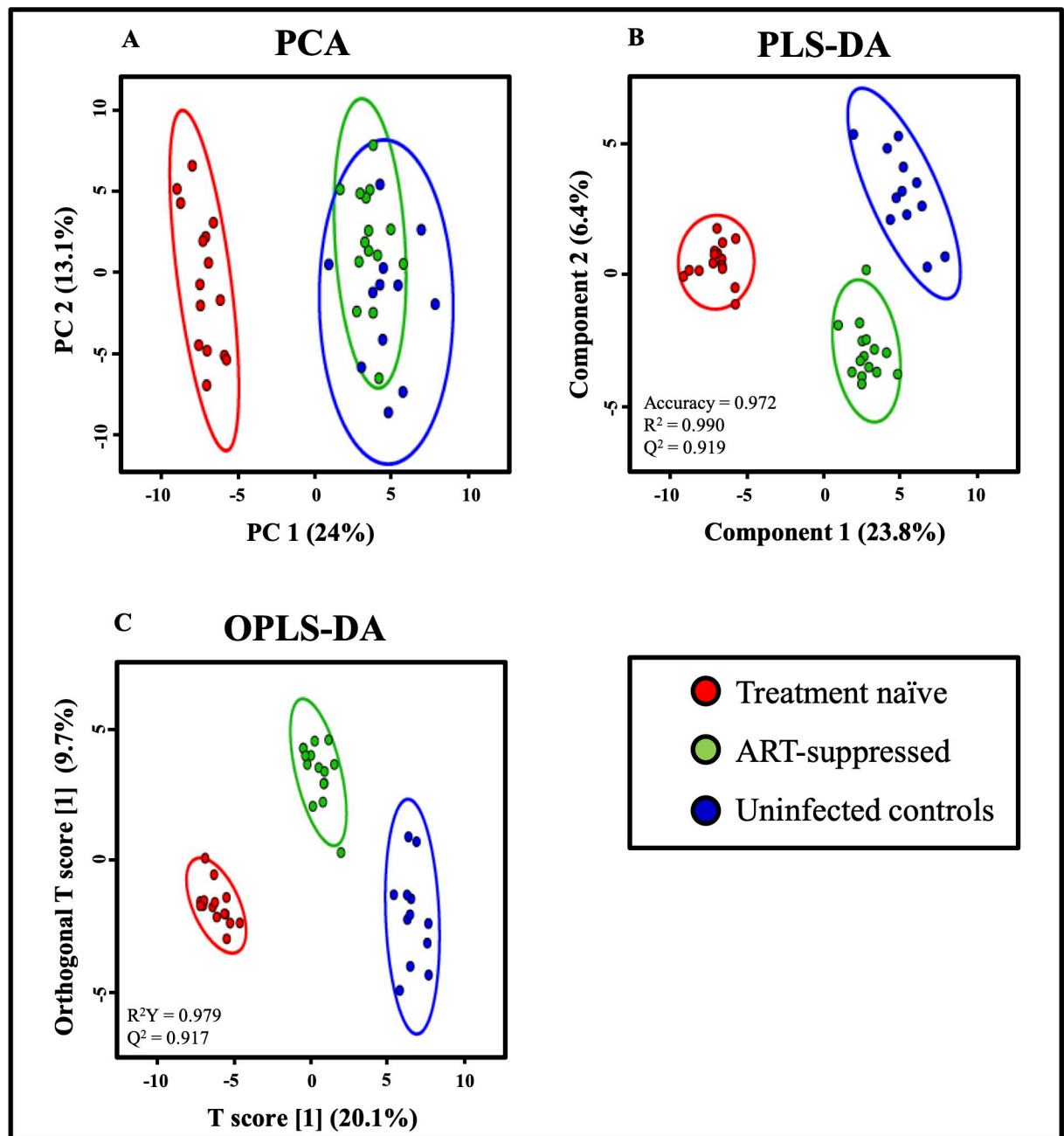
Fig 2. A. PCA B. PLS-DA C. OPLS-DA score plots developed from 1H NMR spectra of plasma of treatment-naïve (red), ART-suppressed (green), perinatally HIV-infected children and uninfected controls (blue). Each dot represents individual samples.

https://doi.org/10.1371/journal.pone.0238316.g002

Interestingly, the use of ART does not seem to have any effect on the perturbed glycolytic pathway. In ART-suppressed HIV-infected children, the glucose level is restored to that of uninfected controls, however, the levels of lactate and phosphoenolpyruvic acid remain elevated despite the suppressive therapy. Hyperlactatemia has been reported in HIV-infected children receiving antiretroviral treatment as well as in ART-exposed HIV uninfected children born to HIV-infected mothers [37, 38]. High plasma lactate concentration is directly associated with insulin resistance and increased hepatic gluconeogenesis in type-2 diabetic subjects
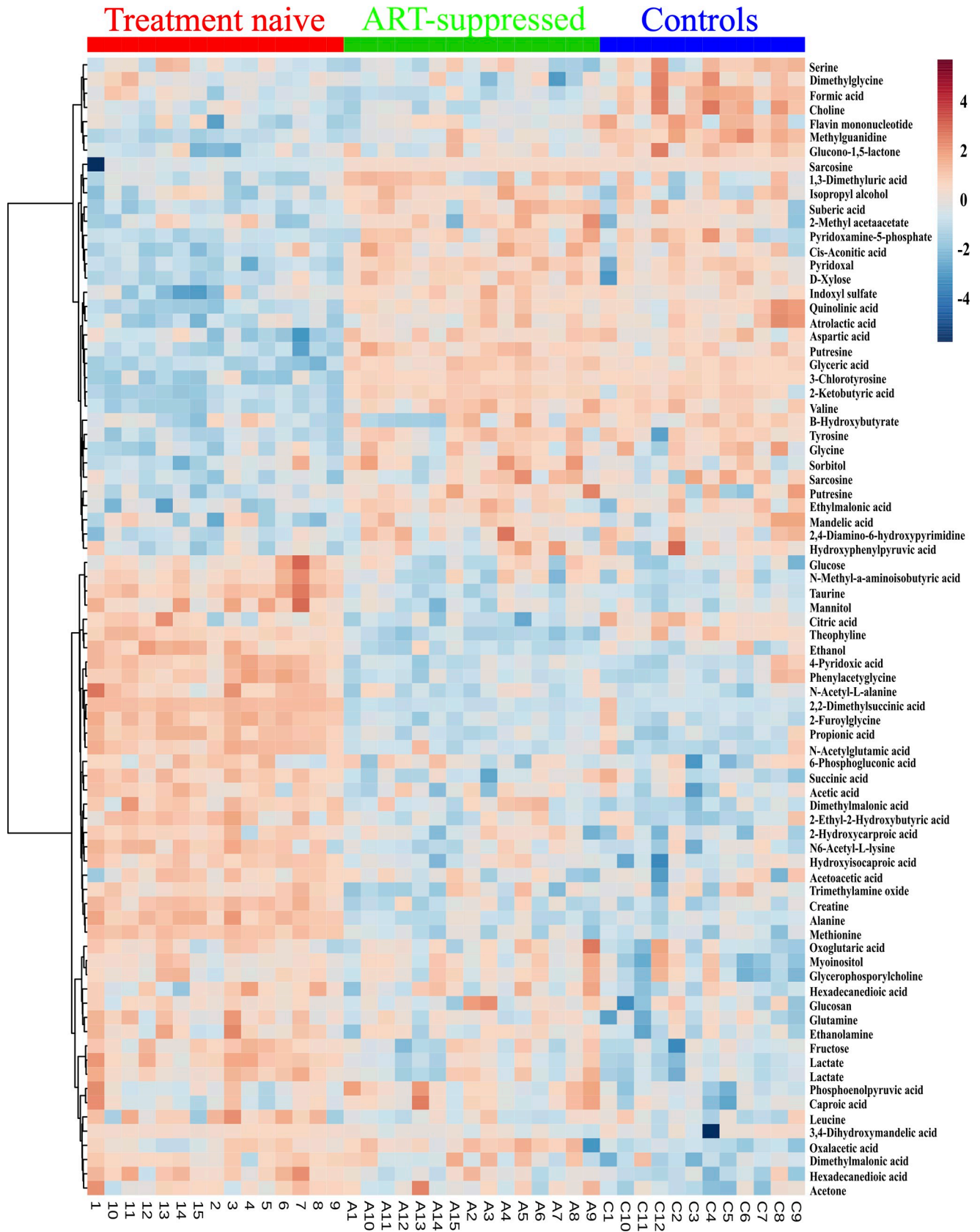
Fig 3. Unsupervised hierarchical clustering of top 75 metabolites that distinguish treatment-naïve, ART-suppressed perinatally HIV infected children from uninfected controls. Each cell in the heat map denotes relative level of metabolites, with samples in column and metabolites in the row. Red and blue indicate increased and decreased levels, respectively.

[39]. Our results of high levels of lactate in treated and untreated perinatally HIV-infected children are in agreement with the previous finding [37, 38, 40] and suggests that perinatally HIV-infected children are at high risk of developing insulin resistance and diabetes even during suppressive treatment.

High level of plasma succinic acid is associated with inflammation as shown in case of cancer [41]. It induces primary inflammatory cytokine, IL-1β, through HIF-1α signaling [42]. Also, when dendritic cells (DCs) were simultaneously primed with both succinate and antigen, T cell activation was increased, as shown by elevated TNF-α and IFN-γ production from these cells [43]. Thus, succinate is an important metabolite that can act as an inflammatory signature. Increased levels of succinic acid in treatment-naïve perinatally HIV-infection children reflect elevated inflammation that appears to normalize during treatment.

We observed elevated levels of plasma TMAO and propionic acid, a gut-microbiome dependent metabolite, in untreated HIV-infected children. Gut microbiota has a significant role in metabolism of host. Gut microbiota is associated with numerous metabolic conditions including diabetes, obesity, and CVD [44, 45]. Choline which comes from dietary phosphatidylcholine is metabolized by gut microbes to trimethylamine (TMA), which further oxidizes to TMAO in liver. Wang et al. showed that the metabolites of dietary phosphatidylcholine promote cardiovascular disease (CVD) [46]. Plasma level of TMAO has been shown to be associated with CVD in general population [47, 48] and carotid artery atherosclerosis progression in HIV-infected adults [49]. This suggests that perinatally HIV-infected children are at the risk of developing CVD. Further, propionic acid, that is synthesized by the gut microbes during complex carbohydrates fermentation in the colon is taken up to the circulation where it further metabolizes in the liver and serves as an energy source. Propionic acid regulates glucose homeostasis and is antiobesogenic [50]. However, elevated levels of propionic acid were reported in obese individuals [51] and also in obese diabetes mice [52], indicating that propionic acid might may pathogenic roles via mechanisms yet to be elucidated. The increase in TMAO and propionic acid level in untreated HIV-infected children might be attributed to the gut dysbiosis as we observed in our previous study [53].

Elevated Myo-inositol among untreated HIV-infected children is similar to earlier reports where they showed myo-inositol to be elevated in left frontal brain of HIV-infected children [54]. Increased myo-inositol in both gray and white matter and also in basal ganglia regions were reported in chronically HIV-infected adults [55, 56]. Myo-inositol is a marker of glial cells and elevated myo-inositol indicates gliosis, a condition of proliferation or hypertrophy of glial cells in response to damage to the central nervous system (CNS). Increased myo-inositol in both treatment-naïve and ART-suppressed HIV-infected children suggests the presence of neuroinflammation and thus might potentially contribute to neurocognitive disorders despite successful virologic control by ART. Previous study has also demonstrated neuroinflammation and cognitive impairment in treated HIV-infected adults [57].

Increased glutamine among untreated HIV-infected children could reflect CD4 T cell skewing and activation and as shown earlier in mice [58]. This was further confirmed by Wang et. al, where glutamine catabolism was shown to be tightly coupled with the biosynthesis of polyamines that are essential for T cell proliferation [59].

A study by Ziegler et al reported decreased levels of plasma amino acids except glutamate in HIV-infected youth [60]. Our study also observed decreased valine, aspartic acid, glycine,
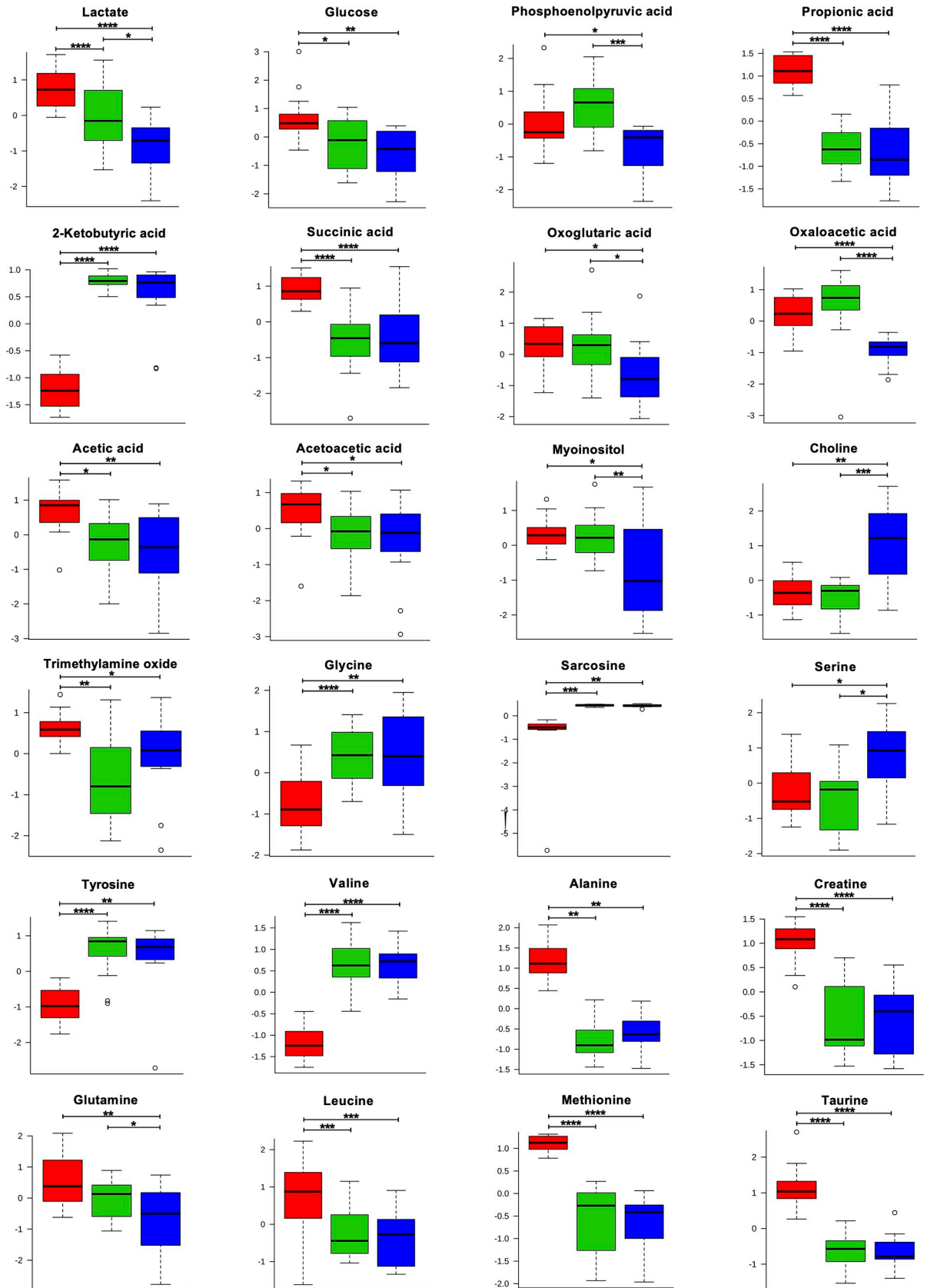
Fig 4. Box plots illustrating the levels of representatives metabolites in the plasma of treatment-naïve (red), ART-suppressed (green) perinatally HIV infected subjects and uninfected controls (blue). The y-axis shows the normalized concentrations of the metabolites. Each box represents interquartile range (IQR) between 25% and the 75% percentiles while the error bar represents 5% and 95% percentiles. Horizontal line within box denotes the median value. Circles indicate the single data points. * = $p < 0.05$, ** = $p < 0.005$, *** = $p < 0.00005$, **** = $p > 0.00005$. $p < 0.05$ was statistically significant.

tyrosine, serine and sarcosine levels in the HIV infected treatment-naïve group. This might be due to intestinal malabsorption as observed in HIV-infected individuals. Intestinal epithelial apoptosis and increased epithelial barrier disruption during chronic HIV infection [61] might reduce amino acids absorption. In addition to nutritional deficit, the change in plasma amino acids levels is also due to alteration in aminoacid metabolic pathway.

In conclusion, our NMR-based metabolomics with an array of robust multivariate statistical techniques have unraveled distinct metabolic phenotypes and pathways among treatment-naïve, ART-suppressed perinatally HIV-infected children and uninfected controls. Untreated and ART-suppressed HIV-infected children had perturbed glycolysis, TCA cycle, aminoacid metabolism. Developing therapeutic strartegies targeting metabolic abnormalities and restoring healthy gut microbiota may be beneficial for preventing diabetes, cardiovascular disease or other associated complication in perinatally HIV-infected children.
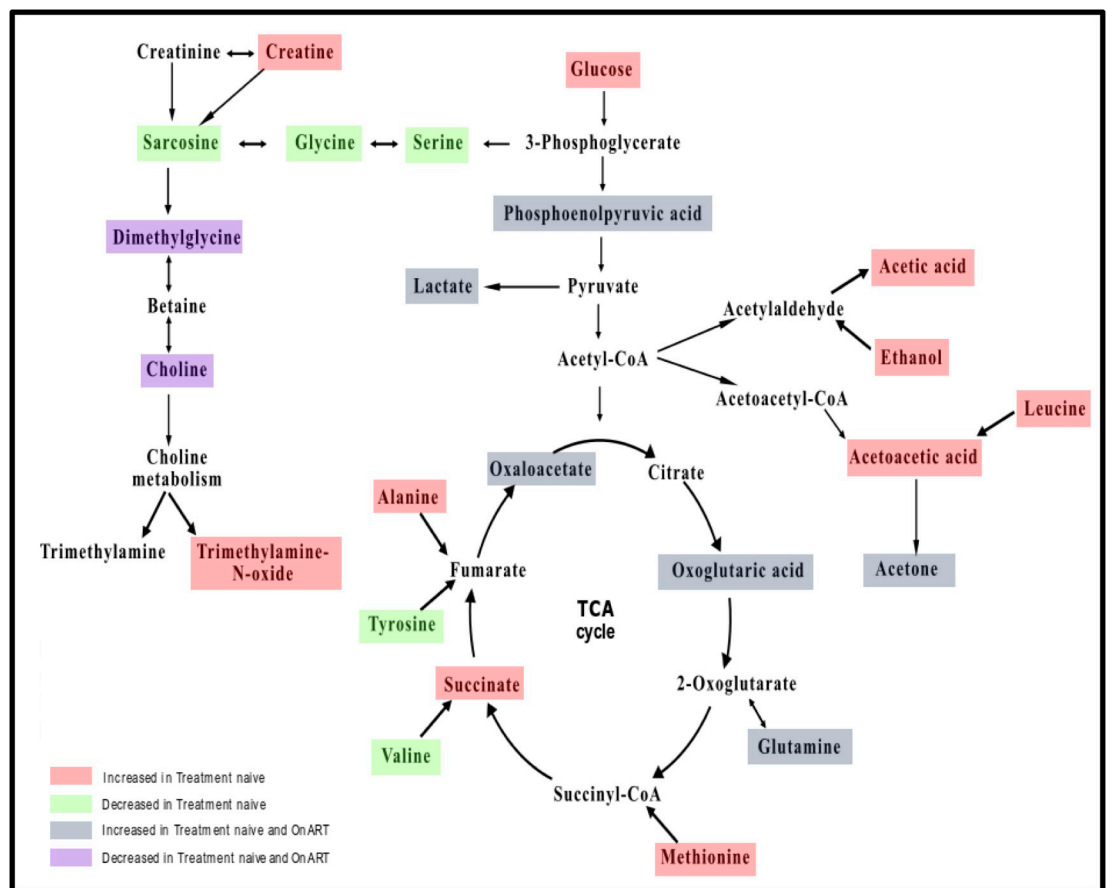

Fig 5. Perturbed metabolic pathways in treatment-naïve and ART-suppressed perinatally HIV infected children.

Supporting information

S1 Fig. The representative 500 MHz 1H-1H J-Resolved (JRes) spectrum. Three different spectral region of the 1D 1H Jres spectrum are expanded for improved visualization: (A) δ (0.0–3.0) ppm, (B) δ (3.0–4.10) ppm and (C) δ (4.80–9.00) ppm. Assigned peaks are annotated. (SVG)

S1 Table. Significantly altered metabolites in treatment naïve and ART-suppressed HIV infected children.
(PDF)

S2 Table. Perturbed metabolic pathways between treatment naïve, ART-suppressed HIV infected children and uninfected controls.
(PDF)

S1 Raw data. Compressed file containing NMR raw data of all study subjects.
(TGZ)

Acknowledgments

Author Contributions

Conceptualization: Anita Shet, Neel Sarovar Bhavesh, Ravi Tandon.

Data curation: Urvinder Kaur S., Bolaji Fatai Oyeyemi.

Formal analysis: Urvinder Kaur S., Bolaji Fatai Oyeyemi.

Funding acquisition: Ravi Tandon.

Investigation: Urvinder Kaur S., Bolaji Fatai Oyeyemi, Bindu Parachalil Gopalan.

Methodology: Urvinder Kaur S.

Resources: Anita Shet, Himanshu D., Neel Sarovar Bhavesh, Ravi Tandon.

Supervision: Neel Sarovar Bhavesh, Ravi Tandon.

Validation: Himanshu D., Neel Sarovar Bhavesh, Ravi Tandon.

Visualization: Urvinder Kaur S.

Writing – original draft: Urvinder Kaur S., Bolaji Fatai Oyeyemi.

Writing – review & editing: Urvinder Kaur S., Bolaji Fatai Oyeyemi, Anita Shet, Bindu Parachalil Gopalan, Himanshu D., Neel Sarovar Bhavesh, Ravi Tandon.

References

1. UNAIDS DATA 2019. 2019. Available: https://www.unaids.org/sites/default/files/media_asset/2019-UNAIDS-data_en.pdf

2. Tobin NH, Aldrovandi GM. Immunology Of Pediatric HIV Infection. Immunol Rev. 2013; 254: 143–169. https://doi.org/10.1111/imr.12074 PMID: 23772619

3. Gona P, Van Dyke RB, Williams PL, Dankner WM, Chernoff MC, Nachman SA, et al. Incidence of opportunistic and other infections in HIV-infected children in the HAART era. J Am Med Assoc. 2006; 296: 292–300. https://doi.org/10.1001/jama.296.3.292 PMID: 16849662

4. Fortuny C, Deyà-Martínez Á, Chiappini E, Galli L, de Martino M, Noguera-Julian A. Metabolic and renal adverse effects of antiretroviral therapy in HIV-infected children and adolescents. Pediatr Infect Dis J. 2015; 34: S36–43. https://doi.org/10.1097/INF.0000000000000663 PMID: 25629891

5. Dapena M, Jiménez B, Noguera-Julian A, Soler-Palacín P, Fortuny C, Lahoz R, et al. Metabolic disorders in vertically HIV-infected children: future adults at risk for cardiovascular disease. J Pediatr Endocrinol Metab. 2012; 25: 529–35. https://doi.org/10.1515/jpem-2012-0005 PMID: 22876550

6. Padmapriyadarsini C, Shet A, Srinivasan R, Ramachandran G, Sanjeeva G, Devi P, et al. High Prevalence of Lipid Abnormalities and Insulin Resistance Among Antiretroviral Naïve HIV-Infected Children in India. Pediatr Infect Dis J. 2017; 37: 253–257. https://doi.org/10.1097/INF.0000000000001829 PMID: 29189659

7. Kumar P, Suri D, Vignesh P, Verma Attri S, Kumar Bhalla A, Singh S. Metabolic Abnormalities and Clinical Lipodystrophy in Children With Human Immunodeficiency Virus Infection: A Report From a Tertiary Care Center in India. Pediatr Infect Dis J. 2017; 36: e313–e316. https://doi.org/10.1097/INF.0000000000001738 PMID: 28787389

8. Ledru E, Christeff N, Patey O, De Truchis P, Melchior JC, Gougeon ML. Alteration of tumor necrosis factor-α T-cell homeostasis following potent antiretroviral therapy: Contribution to the development of human immunodeficiency virus-associated lipodystrophy syndrome. Blood. 2000; 95: 3191–3198. https://doi.org/10.1182/blood.v95.10.3191.010k10_3191_3198 PMID: 10807787

9. Barlow-mosha L, Eckard AR, Mccomsey GA, Musoke PM. Metabolic complications and treatment of perinatally HIV-infected children and adolescents. J Int AIDS Soc. 2013; 16. https://doi.org/10.7448/IAS.16.1.18600 PMID: 23782481

10. Temple ME, Koranyi KI, Nahata MC. Lipodystrophy in HIV-infected pediatric patients receiving protease inhibitors. Ann Pharmacother. 2003; 37: 1214–1218. https://doi.org/10.1345/aph.1A444 PMID: 12921501

11. McComsey GA, O'Riordan M, Hazen SL, El-Bejjani D, Bhatt S, Brennan M-L, et al. Increased carotid intima media thickness and cardiac biomarkers in HIV infected children. Aids. 2007; 21: 921–927. https://doi.org/10.1097/QAD.0b013e328133f29c PMID: 17457085

12. Innes S, Abdullah KL, Haubrich R, Cotton MF, Browne SH. High prevalence of dyslipidemia and insulin resistance in HIV-infected prepubertal African children on antiretroviral therapy. Pediatr Infect Dis J. 2016; 35: e1–e7. https://doi.org/10.1097/INF.0000000000000927 PMID: 26421804

13. Reis LC dos, Rondó PH de C Marques HH de S, Andrade SB de. Dyslipidaemia and insulin resistance in vertically HIV-infected children and adolescents. Trans R Soc Trop Med Hyg. 2011; 105: 197–203. https://doi.org/10.1016/j.trstmh.2011.01.005 PMID: 21371728

14. Grunfeld C, Tien P. Difficulties in Understanding the Metabolic Complications of Acquired Immune Deficiency Syndrome. Clin Infect Dis. 2003; 37: S43–S46. https://doi.org/10.1086/375886 PMID: 12942373

15. Arpadi S, Shiau S, Strehlau R, Martens L, Patel F, Coovadia A, et al. Metabolic abnormalities and body composition of HIV-infected children on Lopinavir or Nevirapine-based antiretroviral therapy. Arch Dis Child. 2013; 98: 258–264. https://doi.org/10.1136/archdischild-2012-302633 PMID: 23220209

16. Jesson J, Dahourou DL, Folquet MA, Malateste K, Yonaba C, N'Gbeche MS, et al. Malnutrition, growth response and metabolic changes within the first 24 months after ART initiation in HIV-infected children treated before the age of 2 years in West Africa. Pediatr Infect Dis J. 2018; 37: 781–787. https://doi.org/10.1097/INF.0000000000001932 PMID: 29406463

17. Brindle JT, Antti H, Holmes E, Tranter G, Nicholson JK, Bethell HWL, et al. Rapid and noninvasive diagnosis of the presence and severity of coronary heart disease using 1H-NMR-based metabonomics. Nat Med. 2002; 8: 1439–1445. https://doi.org/10.1038/nm1202-802 PMID: 12447357

18. Wang H, Wang L, Zhang H, Deng P, Chen J, Zhou B, et al. ^{1}H NMR-based metabolic profiling of human rectal cancer tissue. Mol Cancer. 2013; 12: 1–12. https://doi.org/10.1186/1476-4598-12-1

19. Gabbani T, Marsico M, Bernini P, Lorefice E, Grappone C, Biagini MR, et al. Metabolomic analysis with1H-NMR for non-invasive diagnosis of hepatic fibrosis degree in patients with chronic hepatitis C. Dig Liver Dis. 2017; 49: 1338–1344. https://doi.org/10.1016/j.dld.2017.05.018 PMID: 28625405

20. Hewer R, Vorster J, Steffens FE, Meyer D. Applying biofluid 1H NMR-based metabonomic techniques to distinguish between HIV-1 positive/AIDS patients on antiretroviral treatment and HIV-1 negative individuals. J Pharm Biomed Anal. 2006; 41: 1442–1446. https://doi.org/10.1016/j.jpba.2006.03.006 PMID: 16621406

21. Williams A, Kgoadi K, Steffens F, Steenkamp P, Meyer D. UPLC-MS Metabonomics Reveals Perturbed Metabolites in HIV-Infected Sera. Curr Metabolomics. 2014; 2: 37–52. https://doi.org/10.2174/2213235x02666140214201251

22. Munshi SU, Rewari BB, Bhavesh NS, Jameel S. Nuclear magnetic resonance based profiling of biofluids reveals metabolic dysregulation in HIV-infected persons and those on anti-retroviral therapy. PLoS One. 2013; 8: e64298. https://doi.org/10.1371/journal.pone.0064298 PMID: 23696880

23. Philippeos C, Steffens FE, Meyer D. Comparative 1H NMR-based metabonomic analysis of HIV-1 sera. J Biomol NMR. 2009; 44: 127–137. https://doi.org/10.1007/s10858-009-9329-8 PMID: 19513588

24. Mothi SN, Karpagam S, Swamy VHT, Lala Mamatha M, Sarvode SM. Paediatric HIV—trends & challenges. Indian J Med Res. 2011; 134: 912–919. https://doi.org/10.4103/0971-5916.92636 PMID: 22310823

25. Anigilaje EA, Aderibigbe SA. Mortality in a Cohort of HIV-Infected Children: A 12-Month Outcome of Antiretroviral Therapy in Makurdi, Nigeria. Adv Med. 2018; 2018: 1–11. https://doi.org/10.1155/2018/6409134 PMID: 30018988

26. Xia J, Wishart DS. Using metaboanalyst 3.0 for comprehensive metabolomics data analysis. Curr Protoc Bioinforma. 2016; 2016: 14.10.1–14.10.91. https://doi.org/10.1002/cpbi.11 PMID: 27603023

27. van den Berg RA, Hoefsloot HC, Westerhuis JA, Smilde AK, van der Werf MJ. Centering, scaling, and transformations: improving the biological information content of metabolomics data. BMC Genomics. 2006; 7: 1–15. https://doi.org/10.1186/1471-2164-7-1

28. Wishart DS, Jewison T, Guo AC, Wilson M, Knox C, Liu Y, et al. HMDB 3.0-The Human Metabolome Database in 2013. Nucleic Acids Res. 2013;41. https://doi.org/10.1093/nar/gks1065 PMID: 23161693

29. Nicholson JK, Wilson ID, Fiehn O, Lenz EM, Dettmer K, Aronov PA, et al. Web Server Based Complex Mixture Analysis by NMR. Prog Nucl Magn Reson Spectrosc. 2003; 2: 34. https://doi.org/10.1021/ac702530t PMID: 18422338

30. Ogata H, Goto S, Sato K, Fujibuchi W, Bono H, Kanehisa M. KEGG: Kyoto encyclopedia of genes and genomes. Nucleic Acids Res. 1999; 27: 29–34. https://doi.org/10.1093/nar/27.1.29 PMID: 9847135

31. Aboud M, Elgalib A, Kulasegaram R, Peters B. Insulin resistance and HIV infection: a review. Int J Clin Pract. 2007; 61: 463–472. https://doi.org/10.1111/j.1742-1241.2006.01267.x PMID: 17313615

32. Bugianesi E, McCullough AJ, Marchesini G. Insulin resistance: A metabolic pathway to chronic liver disease. Hepatology. 2005; 42: 987–1000. https://doi.org/10.1002/hep.20920 PMID: 16250043

33. Chimenti MS, Triggianese P, Conigliaro P, Candi E, Melino G, Perricone R. The interplay between inflammation and metabolism in rheumatoid arthritis. Cell Death Dis. 2015; 6: e1887–10. https://doi.org/10.1038/cddis.2015.246 PMID: 26379192

34. Lan X, Cheng K, Chandel N, Lederman R, Jhaveri A, Husain M, et al. High glucose enhances HIV entry into T cells through upregulation of CXCR4. J Leukoc Biol. 2013; 94: 769–77. https://doi.org/10.1189/jlb.0313142 PMID: 23911867

35. Shanmugam N, Reddy MA, Guha M, Natarajan R. High glucose-induced expression of proinflammatory cytokine and chemokine genes in monocytic cells. Diabetes. 2003; 52: 1256–1264. https://doi.org/10.2337/diabetes.52.5.1256 PMID: 12716761

36. Mikulak J, Oriolo F, Portale F, Tentorio P, Lan X, Saleem MA, et al. Impact of APOL1 polymorphism and IL-1β priming in the entry and persistence of HIV-1 in human podocytes. Retrovirology. 2016; 13: 1. https://doi.org/10.1186/s12977-015-0234-9

37. Soler-Palacín P, Martín-Nalda A, Martínez-Gómez X, Melendo S, Riudor E, Arranz JA, et al. Hyperlactatemia and in Utero Exposure to Antiretrovirals: Is the Control Group the Clue? AIDS Res Hum Retroviruses. 2011; 28: 752–758. https://doi.org/10.1089/AID.2011.0198 PMID: 22010980

38. Ramshorst MS Van, Struthers HE, Mcintyre JA, Chb MB. Blood Lactate in HIV-infected Children on Antiretroviral Therapy in Rural South Africa Characteristics of Study Population. 2014; 33: 393–395. https://doi.org/10.1097/INF.0000000000000036 PMID: 23995586

39. Brinkmann C, Brixius K. Hyperlactatemia in type 2 diabetes: Can physical training help? Journal of Diabetes and its Complications. Elsevier Inc.; 2015. pp. 965–969. https://doi.org/10.1016/j.jdiacomp.2015.05.018 PMID: 26122286

40. Noguera A, Fortuny C, Mun C. Hyperlactatemia in Human Immunodeficiency Virus–Uninfected Infants Who Are Exposed to Antiretrovirals. AIDS Res Hum Retroviruses. 2017; 28. https://doi.org/10.1542/peds.2004-0955 PMID: 15492359

41. Zhao T, Mu X, You Q. Succinate: An initiator in tumorigenesis and progression. Oncotarget. 2017; 8: 53819–53828. https://doi.org/10.18632/oncotarget.17734 PMID: 28881853

42. Tannahill GM, Curtis AM, Adamik J, Palsson-Mcdermott EM, McGettrick AF, Goel G, et al. Succinate is an inflammatory signal that induces IL-1β through HIF-1α. Nature. 2013; 496: 238–242. https://doi.org/10.1038/nature11986 PMID: 23535595

43. Rubic T, Lametschwandtner G, Jost S, Hinteregger S, Kund J, Carballido-Perrig N, et al. Triggering the succinate receptor GPR91 on dendritic cells enhances immunity. Nat Immunol. 2008; 9: 1261–1269. https://doi.org/10.1038/ni.1657 PMID: 18820681

44. Mazidi M, Rezaie P, Kengne AP, Mobarhan MG, Ferns GA. Gut microbiome and metabolic syndrome. Diabetes Metab Syndr Clin Res Rev. 2016; 10: S150–S157. https://doi.org/10.1016/j.dsx.2016.01.024 PMID: 26916014

45. Tang WHW, Kitai T, Hazen SL. Gut microbiota in cardiovascular health and disease. Circ Res. 2017; 120: 1183–1196. https://doi.org/10.1161/CIRCRESAHA.117.309715 PMID: 28360349

46. Wang Z, Klipfell E, Bennett BJ, Koeth R, Levison BS, Dugar B, et al. Gut flora metabolism of phosphatidylcholine promotes cardiovascular disease. Nature. 2011; 472: 57–65. https://doi.org/10.1038/nature09922 PMID: 21475195

47. Trøseid M, Ueland T, Hov JR, Svardal A, Gregersen I, Dahl CP, et al. Microbiota-dependent metabolite trimethylamine-N-oxide is associated with disease severity and survival of patients with chronic heart failure. J Intern Med. 2015; 277: 717–726. https://doi.org/10.1111/joim.12328 PMID: 25382824

48. Stubbs JR, House JA, Ocque AJ, Zhang S, Johnson C, Kimber C, et al. Serum Trimethylamine-N-Oxide is Elevated in CKD and Correlates with Coronary Atherosclerosis Burden. J Am Soc Nephrol. 2016; 27: 305–313. https://doi.org/10.1681/ASN.2014111063 PMID: 26229137

49. Shan Z, Clish CB, Hua S, M. SJ, B. HD, D. BR, et al. Gut microbial-related choline metabolite trimethylamine-N-oxide is associated with progression of carotid artery atherosclerosis in HIV infection. J Infect Dis. 2018; 218: 1474–1479. https://doi.org/10.1093/infdis/jiy356 PMID: 29912352

50. Al-Lahham SH, Peppelenbosch MP, Roelofsen H, Vonk RJ, Venema K. Biological effects of propionic acid in humans; metabolism, potential applications and underlying mechanisms. Biochimica et Biophysica Acta—Molecular and Cell Biology of Lipids. Elsevier B.V.; 2010. pp. 1175–1183. https://doi.org/10.1016/j.bbalip.2010.07.007 PMID: 20691280

51. Schwiertz A, Taras D, Schäfer K, Beijer S, Bos NA, Donus C, et al. Microbiota and SCFA in lean and overweight healthy subjects. Obesity. 2010; 18: 190–195. https://doi.org/10.1038/oby.2009.167 PMID: 19498350

52. Nishitsuji K, Xiao J, Nagatomo R, Umemoto H, Morimoto Y, Akatsu H, et al. Analysis of the gut microbiome and plasma short-chain fatty acid profiles in a spontaneous mouse model of metabolic syndrome. Sci Rep. 2017; 7: 1–10. https://doi.org/10.1038/s41598-016-0028-x

53. Kaur US, Shet A, Rajnala N, Gopalan BP, Moar P, D H, et al. High Abundance of genus Prevotella in the gut of perinatally HIV-infected children is associated with IP-10 levels despite therapy. Sci Rep. 2018; 8: 1–16. https://doi.org/10.1038/s41598-017-17765-5 PMID: 29311619

54. Banakar S, Thomas MA, Deveikis A, Watzl JQY, Hayes J, Keller MA. Two-dimensional1H MR spectroscopy of the brain in human immunodeficiency virus (HIV)-infected children. J Magn Reson Imaging. 2008; 27: 710–717. https://doi.org/10.1002/jmri.21251

55. Chang L, Ernst T, Witt MD, Ames N, Gaiefsky M, Miller E. Relationships among brain metabolites, cognitive function, and viral loads in antiretroviral-naïve HIV patients. Neuroimage. 2002; 17: 1638–1648. https://doi.org/10.1006/nimg.2002.1254 PMID: 12414302

56. Letendre SL, Zheng JC, Kaul M, Yiannoutsos CT, Ellis RJ, Taylor MJ, et al. Chemokines in cerebrospinal fluid correlate with cerebral metabolite patterns in HIV-infected individuals. J Neurovirol. 2011; 17: 63–69. https://doi.org/10.1007/s13365-010-0013-2 PMID: 21246320

57. Harezlak J, Buchthal S, Taylor M, Schifitto G, Zhong J, Daar E, et al. Persistence of HIV-associated cognitive impairment, inflammation, and neuronal injury in era of highly active antiretroviral treatment. Aids. 2011; 25: 625–633. https://doi.org/10.1097/QAD.0b013e3283427da7 PMID: 21297425

58. Klysz D, Tai X, Robert PA, Craveiro M, Cretenet G, Oburoglu L, et al. Glutamine-dependent α-ketoglutarate production regulates the balance between T helper 1 cell and regulatory T cell generation. Sci Signal. 2015; 8. https://doi.org/10.1126/scisignal.aab2610 PMID: 26420908

59. Wang R, Dillon CP, Shi LZ, Milasta S, Carter R, Finkelstein D, et al. The Transcription Factor Myc Controls Metabolic Reprogramming upon T Lymphocyte Activation. Immunity. 2011; 35: 871–882. https://doi.org/10.1016/j.immuni.2011.09.021 PMID: 22195744

60. Ziegler TR, Judd SE, Ruff JH, McComsey GA, Eckard AR. Amino Acid Concentrations in HIV-Infected Youth Compared to Healthy Controls and Associations with CD4 Counts and Inflammation. AIDS Res Hum Retroviruses. 2017; 33: 681–689. https://doi.org/10.1089/AID.2015.0369 PMID: 28117597

61. Epple H-J, Zeitz M. HIV infection and the intestinal mucosal barrier. Ann N Y Acad Sci. 2012; 1258: 19–24. https://doi.org/10.1111/j.1749-6632.2012.06512.x PMID: 22731711